Influence of mediated processes on the removal of Rhodamine with CDEO

Danyelle Medeiros de Araújo[1], Cristina Sáez [2], Carlos A. Martínez-Huitle[1,*], Pablo Cañizares[2], M. A. Rodrigo[2]

[1] Institute of Chemistry, Federal University of Rio Grande do Norte, Lagoa Nova CEP 59078-970, Natal, RN, Brazil

[2]Department of Chemical Engineering. Enrique Costa Building. Campus Universitario s/n. 13071 Ciudad Real. Spain

Abstract

The influence of the mediated oxidation on the removal of Rhodamine B (xanthene dye) solutions with conductive-diamond electrochemical oxidation (CDEO) is studied. To do this, four different supporting electrolytes have been used: Na_2SO_4, $HClO_4$, H_3PO_4, NaCl. Total removal of organic pollutants is attained with CDEO regardless of the supporting electrolyte media used, although media clearly influences on efficiency and rate of the processes. Sulfate and phosphate media show a similar behavior, whereas electrolysis in perchlorate media behaves surprisingly better than chloride media. Current density is playing an important role. In all cases, CDEO follows a first order kinetic (linear trend in semi logarithmic plot) and kinetic constants are generally much greater than expected according to a single mass transfer electrolytic model. This is not the expected result for a direct electrochemical oxidation process and it indicates the importance of mediated electrochemical processes in the removal of Rhodamine B. The harsh oxidation conditions of CDEO leads to the formation of less reaction

intermediates than other technologies. The presence of short chain aliphatic acids is discharted, and the intermediates (aromatic acids) formed during the initial stages of the process are rapidly mineralized to carbon dioxide. In chloride media, chlorinated intermediates are also formed by the action of hypochlorite.

Key Words: Electrochemical oxidation**,** diamond**,** dyes, mediated oxidation, supporting electrolyte.

* Corresponding author:

1. Introduction

The treatment of textile effluents has given much attention in the last years because the discharge of highly pigmented synthetic dyes to the ecosystem causes significant damage to aquatic and human lives (Carneiro et al., 2010). Conventional technologies are inefficient to remove these organics due to the high water solubility of dyes (in the case of using coagulation and precipitation (Muthukumar et al., 2005)), and to the typical pH and salt concentration of dye effluents (in the case of using biological methods (Pandey et al., 2007). In this point, Advanced Oxidation Processes appears as a good alternative for the treatment of synthetic dyes effluents. Among them, Fenton oxidation (Cruz-Gonzalez et al., 2012; Panizza and Cerisola, 2009b), photocatalysis (He et al., 2009; Miller et al., 2013), sonochemical degradation (Guzman-Duque et al., 2011; Merouani et al., 2010) and electrochemical oxidation (Martinez-Huitle et al., 2012; Rocha et al., 2012; Saez et al., 2007; Tavares et al., 2012) have been widely studied in literature for the treatment of a great variety of dyes. In general, these technologies are able to attain very good results in terms of decolorization due to the rapid cleavage of chromophore group of the dye molecule. However, mineralization efficiency shows a marked influence of the oxidative capacity of each degradation technology. Generally, aromatic and aliphatic acids are the main intermediates detected during dye degradation process, although their maximum concentration depends on the conditions used in each case. In this point, recent works have shown that electrochemical oxidation, and in particular Conductive Diamond Electrochemical Oxidation (CDEO), can be successfully applied with high organic removal rates and without important operational limitations (Aquino et al., 2013; Aquino et al., 2012; Faouzi et al., 2006; Ramirez et al., 2013; Saez et al., 2007). The harsh oxidation conditions attained with CDEO are explained in terms of the oxidation mechanisms involved in the process. In this way, it

is well documented that during CDEO a noteworthy production of hydroxyl radicals in the nearness of diamond surfaces takes place. These radicals are fully available for oxidizing reactions but their lifetime is very short and not enough to let them diffuse to the bulk solution. Thus, the action of these radicals is limited to the short region close to the electrode surface where they are produced, and the kinetic of these processes is usually controlled by mass transport. Additionally, it is well documented the availability of CDEO to produce inorganic oxidants, which are difficult or even impossible to be produced with other different anodic materials, from the oxidation of supporting electrolyte (Cañizares et al., 2005a; Cañizares et al., 2009; Sáez et al., 2008). In fact, some works have also been focused on the electrochemical synthesis with diamond anodes of powerful oxidants such as persulfates (Serrano et al., 2002), perphosphates (Cañizares et al., 2005a), perchlorates (Bergmann et al., 2014; Sánchez-Carretero et al., 2011) and hypochlorite (Cañizares et al., 2009; Vacca et al., 2011). Thus, besides direct electrooxidation on the surface and oxidation by means of hydroxyl radicals in a region close to the electrode surface, the oxidation mediated by other oxidants electrogenerated on the diamond surface from the electrolyte salts should be taken into account, as it seems to increase the global oxidation efficiency (Aquino et al., 2012; Cañizares et al., 2005b; Panizza and Cerisola, 2009a; Rodrigo et al., 2010).

The dye under consideration is RhB. It is widely used in textiles, leathers and food stuffs with high water solubility (Hou et al., 2011; Miller et al., 2013). Thus, this work focuses on the CDEO of synthetic Rhodamine B (selected as model of xanthene dyes with very good stability) solutions in different supporting media in order to increase the understanding of the role of mediated oxidation on the degradation process.

2. Materials and methods

2.1. Chemicals

Rhodamine was supplied by Sigma-Aldrich Laborchemikalien GmbH (Steinheim, Germany). Anhydrous sodium sulphate, sodium chloride, perchloric acid and phosphoric acid, used as supporting electrolytes, were analytical grade purchased from Fluka. All solutions were prepared with high-purity water obtained from a Millipore Milli-Q system, with resistivity > 18 MΩ cm at 25 ºC. Sulphuric acid and sodium hydroxide used to adjust the solution pH were analytical grade and supplied by Panreac Química S.A. (Barcelona, Spain).

2.2. Analytical procedures

The Total Organic Carbon concentration was monitored using a Multi N/C 3100 Analytik Jena analyzer. Measurements of pH and conductivity were carried out with an InoLab WTW pH-meter and a GLP 31 Crison conductimeter, respectively. The concentrations of the compounds were quantified by HPLC (Agilent 1100 series). The detection wavelength used to detect dye was 248 nm. The column temperature was 25 ºC. Volume injection was set to 50 μL. The analytical column used was Phenomenex Gemini 5 μm C18. The mobile phases were 0.9 ml of 98% formic acid in milli-Q water for analysing intermediates. Samples extracted from electrolyzed solutions were filtered with 0.20 μm Nylon filters before analysis. Moreover, the acids intermediates formed during the experiments were detected with a detection wavelength of 190 nm.

Samples of anolyte were extracted into non-aqueous medium (2 mL of acetonitrile HPLC grade with 20 μL of electrolysis sample) and were subjected to GC-MS analysis using GC-FOCUS and MS-ISQ Thermo Scientific to identify the intermediates following the conditions: GC: Varian column VF5 ms with a composition of 5% de fenil-arylene and 95% de dimetilpolisiloxane. Temperature program: 40ºC – 5 min;

12°C/min – 100ºC; 10ºC/min – 200 ºC and 10ºC/min - 270 ºC – 5 min. Injector: 220ºC. Mode: Splitless. Gas flow: 0.8 mL/min. MS: Transfer line: 270ºC; ions source temperature: 220ºC, Mass range: 40-500 m/z. Injection: 1µL.

2.3. Electrochemical cells

Electrolyses were carried out in a single compartment electrochemical flow cell working under a batch-operation mode (Cañizares et al., 2005b). Conductive –Diamond Electrodes (p-Si–boron-doped diamond) were used as anode and a stainless steel (AISI 304) as cathode. Both electrodes were circular (100 mm diameter) with a geometric area of 78 cm^2 and an electrode gap of 9 mm. Boron-doped diamond films were provided by Adamant Technologies (Neuchatel, Switzerland) and synthesized by the hot filament chemical vapour deposition technique (HF CVD) on single-crystal p-type Si <100> wafers (0.1 Ωcm, Siltronix).

2.4. Experimental procedures

Bench-scale electrolyses of 1000 cm^3 of wastewater were carried out under galvanostatic conditions. The current density employed ranged from 15-120 mA cm^{-2}. The cell voltage did not vary during electrolysis, indicating that conductive-diamond layers did not undergo appreciable deterioration or passivation phenomena. Prior to use in galvanostatic electrolysis assays, the electrode was polarized during 10 min in a 0.035 M Na_2SO_4 solution at 15 mA cm^{-2} to remove any kind of impurity from its surface.

The wastewater consisting of 100 mg dm^{-3} of Rhodamine B and different electrolytes (Na_2SO_4, $HClO_4$, H_3PO_4, NaCl) was stored in a glass tank and circulated through the electrolytic cell by means of a centrifugal pump (flow rate 21.4 dm^3 h^{-1}). A heat

exchanger coupled with a controlled thermostatic bath (Digiterm 100, JP Selecta, Barcelona, Spain) was used to maintain the temperature at the desired set point (25 ºC).

3. Results and discussion

Figure 1 shows the progress of the mineralization during electrolyses at two large current densities (60 and 120 mA cm^{-2}) of synthetic wastewater consisting of aqueous solutions containing 100 mg dm^{-3} of Rhodamine B (RhB) and different electrolytes (Na_2SO_4, $HClO_4$, H_3PO_4, NaCl). As it can be observed, total removal of organic pollutants can be attained with CDEO regardless of the supporting electrolyte media used, although media clearly influences on efficiency and rate of the processes, and current density is playing an important role. This is interesting because it confirms that CDEO is robust enough to deplete pollution but it also informs about the occurrence of different mechanisms of oxidation that should be related with the supporting media. Thus, although chloride media could be expected to show the best results because of the well-known production of chlorine (and then of hypochlorite and hypochloric acid), it attains the worst results and, in fact, it is the only case in which the complete mineralization is not attained for a current charge applied of 100 Ah dm^{-3}. This behavior can be attributed to an interaction between hydroxyl radicals and Cl^- (chloride acts as scavenger of $^{\bullet}OH$) to form different active chlorine species on BDD surface (Bergmann et al., 2009; Cañizares et al., 2009; Sánchez-Carretero et al., 2011) with this non-active material and to the formation of refractory species by chlorination. At the same time, the chloride concentration in the solution can also promote the importance of Cl_2 production at BDD surface, decreasing the Cl^-, and consequently, the production of active chlorine species.

A very interesting observation is the effect of current density in the perchlorate test that shifts towards higher efficiencies at higher current densities. Initially, it is strange because in that media no oxidants production is expected and perchlorate is not a good oxidant at room temperature so, it is not expected to participate in the oxidation. However, higher concentration of hydroxyl radicals are produced under these experimental conditions as well as it can be related to the nature of the hydroxyl radicals produced at different non-active anodes, as already proposed by Bejan and co-workers (Bejan et al., 2012). On the other hand, sulfate and phosphate media show a similar behavior in both current densities tested.

Figure 2 shows a semi-logarithmic plot of the COD decay with the current charge for the same current densities shown in Figure 1. As it can be observed, except for an abrupt decrease during the very first stages of the electrolysis of the synthetic wastewater with chloride media, all tests follow a clear linear trend suggesting that they can be modeled with a first order kinetic, as they were carried out under galvanostatic conditions. This divergence can be explained in terms of the masking effects of chlorides on the measurement of COD. Not great differences are obtained if results of the electrolyses of sulfate and phosphate media are compared. In fact, results with these two supporting electrolytes do not seem to depend on the current density and on the applied charge. However, as it was forwarded by the changes in the mineralization, perchlorate removal rate increases very importantly when current density increases. The same can be observed in the electrolysis in chloride media.

To better observe this influence of the supporting media and current density, and taking into account the linear trend observed in COD decay vs. Q, experimental results of each test were fitted to a first order kinetic decay. Figure 3 shows the influence of the

supporting media and applied current density on the value of these first order kinetic constants for COD removal. These constants were calculated from the slope of semi-logarithmic vs. time plots.

For the case of NaCl, the points corresponding to the first oxidation stage (which fit well to this trend) were used to fit the constant, whereas for the rest of supporting electrolytes the complete set of data was used. The increase of kinetic constants with the applied current density is more important from current densities above 100 mA cm^{-2}. This is the expected behavior of a process with a significant contribution of mediated electrooxidation: the higher the current density, the higher the production of mediated electro-reagents and, hence, the higher the kinetic constant. The lower values obtained in the electrolysis carried out with sodium chlorine as supporting electrolyte can be related to the importance of Cl_2 production at BDD surface, decreasing the production of active chlorine species, and consequently, disfavoring the oxidation of organic matter. In addition, it is important to notice that calculated kinetic constants are much greater than the value expected for a purely mass transfer controlled process (around 0.01 min^{-1}), mainly in the case of working at 120 mA cm^{-2}. This value was calculated from a ferro-ferricyanide standard test carried out with the same experimental setup and under the same flow conditions (Aquino et al., 2012). This certifies that mediated oxidation carried out by electrogenerated oxidants in bulk region plays an important role in the degradation of RhB and mineralization process.

Efficiency of electrolytic processes can be discussed in terms of different parameters such as ICE, ACE, etc. However, in case of a good fitting of results in galvanostatic experiments to a first order kinetics (as it is the case of the results obtained in this work),

it can be demonstrated that efficiency depends linearly on the COD concentration and the constant can be easily calculated from the kinetic constant as reported in literature (Aquino et al., 2014). This constant is of a great importance because it gives directly the value of the efficiency (% of the applied current used in oxidizing organics) if multiplied by the COD (mg dm^{-3}) and in the authors' opinion is the most interesting efficiency parameter to characterize CDEO processes. Figure 4 shows the changes in this parameter for the four supporting electrolytes and current densities assessed. As it can be observed, efficiency decreases as the current density increases, although it increases slightly at high current density (above 100 $mAcm^{-2}$).

Other important point to be studied is the production of intermediates, because some of them can be even more hazardous than the initial pollutant. Their relative concentration and trend can help to increase the understanding of the process. Figure 5 shows the chromatografic area of the main intermediates obtained during the electrolyses at 60 mA cm^{-2} of RhB solutions containing different supporting electrolytes. The cromatographic area of the peak corresponding to RhB has been also included for the sake of comparison. As it can be observed, the harsh oxidation conditions of electrochemical oxidation do not favor the production of many intermediates (only three intermediates seems to be formed in significant concentration), except in the case of NaCl media in which a very rapid depletion of RhB molecule is observed together with the production of seven compounds that clearly behaves as intermediates. Their formation can be related to the attack of ClO^- electrochemically generated by oxidation of Cl^- to RhB molecule. This observation can explain the trend observed in COD decay during the electrolysis of RhB in chloride media. However, in all cases, intermediate concentrations should be very small as compared to that of RhB. As an indication, the

chromatographic area of the RhB peak (with a concentration of 100 mg dm^{-3}) was around 170.000 units, while the maximum response measured for intermediates during the experiments is below 25.000 units for i_2 and below 5.000 units for the rest of intermediates.

Restricting now our analysis to the intermediates produced and identified, a lower amount of intermediates (Phthalic acid (▲); 2,5-Hydroxybenzoic acid (●) and Benzoic acid (■), with low-units of chromatographic area) is produced when $HClO_4$ is used as supporting electrolyte, being completely oxidized after 300 min of electrolysis (Fig. 5a). For the case of H_3PO_4 and Na_2SO_4, the same intermediates were identified (Figs. 5a, 5c and 5d); however, the concentration of them is very different than those obtained to $HClO_4$. An important observation is the significant concentration produced of 2,5-hydroxybenzoic acid when $HClO_4$, H_3PO_4 and Na_2SO_4 are used as supporting electrolytes (Fig. 5a, 5c and 5d) while the concentration of the other intermediates is minor (phthalic acid (▲) and benzoic acid (■), respectively). However, the production of 2,5-hydroxybenzoic acid indicates that RhB is fragmented to form benzoic acid, which is successively oxidized to 2,5-hydroxybenzoic acid, justifying its higher concentration. Then, RhB is preferentially oxidized by strong oxidants (hydroxyl radicals and persulfates/ peroxodiphosphates) produced at BDD surface. These intermediates are completely eliminated after 300 min, in all cases.

On contrary, for NaCl, seven sub-products are produced (phthalic acid (▲); 2,5-hydroxybenzoic acid (●); benzoic acid (■); 3-dinitrobenzoic acid (♦); α- hidroxyglutaric acid (△); intermediate 6 (○) and intermediate 7 (□)) when RhB was electrochemically oxidized. No complete elimination of all intermediates formed was accomplished after 500 min of electrolysis, but lower concentration of them remains in solution as showed

by minor chromatographic areas recorded. This fact may be explained by the effective attack of hydroxyl radicals and active chlorine species produced at NaCl media to RhB.

Figure 6 shows the maximum relative chromatographic area of the intermediates generated at different applied current density and supporting media. Comparing results, neither current density nor supporting media influence significantly in the maximum concentration of each intermediate, except in the case of chlorine media in which chlorinated intermediates in lower relative concentration seem to be produced (intermediate 6 (○) and intermediate 7 (□)). At the light of these results, CDEO leads to the formation of less reaction intermediates than other technologies such as photocatalysis degradation (He et al., 2009; Yu et al., 2009; Sun et al., 2009) and Fenton oxidation (Hou et al., 2011) in which benzoic and phtalic acids, aliphatic acids (mainly adipic and glutaric acids) and alcohols of short chain are formed in relevant concentrations. In this case, short chain intermediates are not detected (at least with the analytical method used). The strong oxidation conditions of this technology favor the mineralization of principal intermediates into carbon dioxide and refractory species are not formed in any case.

4. Conclusions

From this work the following conclusions can be drawn:

- RhB can be successfully removed using conductive-diamond electrochemical oxidation regardless of the supporting electrolyte media, although media clearly influences on efficiency and rate of the processes, and current density is playing an important role.

– Kinetic constants are much greater than the value expected for a purely mass transfer controlled process, indicating that there is a significant contribution of mediated oxidation processes. Current density promotes the formation of mediators and rate of the electrolysis improves with increasing this parameter. Opposite efficiency decreases with an increase in current density.

– The harsh oxidation conditions of CDEO favor the rapid mineralization of RhB into carbon dioxide. Aromatics intermediates (mainly phthalic acid and benzoic acids) formed by the cleavage of RhB molecule are the only intermediates detected in the first stages of the degradation process. Neither short chain intermediates nor refractory species are formed in any case. In case of chloride media, chlorinated intermediates can be formed by the attack of hypochlorite to organic compounds.

Acknowledgements

D.M.A. acknowledges CAPES for PhD fellowship and CNPq for the scholarship given for “doutorado sanduiche” under “Ciências sem Fronteiras” program to develop the experimental research at the UCLM-Spain. This work has been supported by the Spanish Government through the project CTM2013-45612-R and EU through project FEDER 2007-2013 PP201010 (Planta Piloto de Estación de Regeneración de Aguas Depuradas).

References

Aquino, J. M., R. C. Rocha-Filho, M. A. Rodrigo, C. Sáez, and P. Cañizares, 2014, High efficiencies in the electrochemical oxidation of an anthraquinonic dye with conductive-diamond anodes, Environmental Science Pollution Research, DOI 10.1007/s11356-014-2784-0.

Aquino, J. M., R. C. Rocha-Filho, M. A. Rodrigo, C. Sáez, and P. Cañizares, 2013, Electrochemical degradation of the Reactive Red 141 dye using a boron-doped diamond anode: Water, Air, and Soil Pollution, v. 224.

Aquino, J. M., M. A. Rodrigo, R. C. Rocha-Filho, C. Sáez, and P. Cañizares, 2012, Influence of the supporting electrolyte on the electrolyses of dyes with conductive-diamond anodes: Chemical Engineering Journal, v. 184, p. 221-227.

Bejan, D., E. Guinea, and N. Bunce, 2012, On the nature of the hydroxyl radicals produced at boron-doped diamond and Ebonex (R) anodes: Electrochimica Acta, v. 69, p. 275-281.

Bergmann, M., A. Koparal, and T. Iourtchouk, 2014, Electrochemical Advanced Oxidation Processes, Formation of Halogenate and Perhalogenate Species: A Critical Review: Critical Reviews in Environmental Science and Technology, v. 44, p. 348-390.

Bergmann, M., J. Rollin, and T. Iourtchouk, 2009, The occurrence of perchlorate during drinking water electrolysis using BDD anodes: Electrochimica Acta, v. 54, p. 2102-2107.

Carneiro, P., D. Oliveira, G. Umbuzeiro, and M. Zanoni, 2010, Mutagenic activity removal of selected disperse dye by photoeletrocatalytic treatment: Journal of Applied Electrochemistry, v. 40, p. 485-492.

Cañizares, P., F. Larrondo, J. Lobato, M. A. Rodrigo, and C. Sáez, 2005a, Electrochemical synthesis of peroxodiphosphate using boron-doped diamond anodes: Journal of the Electrochemical Society, v. 152, p. D191-D196.

Cañizares, P., J. Lobato, R. Paz, M. A. Rodrigo, and C. Sáez, 2005b, Electrochemical oxidation of phenolic wastes with boron-doped diamond anodes: Water Research, v. 39, p. 2687-2703.

Cañizares, P., C. Sáez, A. Sánchez-Carretero, and M. A. Rodrigo, 2009, Synthesis of novel oxidants by electrochemical technology: Journal of Applied Electrochemistry, v. 39, p. 2143-2149.

Cruz-Gonzalez, K., O. Torres-Lopez, A. Garcia-Leon, E. Brillas, A. Hernandez-Ramirez, and J. Peralta-Hernandez, 2012, Optimization of electro-Fenton/BDD process for decolorization of a model azo dye wastewater by means of response surface methodology: Desalination, v. 286, p. 63-68.

Faouzi, M., P. Cañizares, A. Gadri, J. Lobato, B. Nasr, R. Paz, M. A. Rodrigo, and C. Saez, 2006, Advanced oxidation processes for the treatment of wastes polluted with azoic dyes: Electrochimica Acta, v. 52, p. 325-331.

Guzman-Duque, F., C. Petrier, C. Pulgarin, G. Penuela, and R. Torres-Palma, 2011, Effects of sonochemical parameters and inorganic ions during the sonochemical degradation of crystal violet in water: Ultrasonics Sonochemistry, v. 18, p. 440-446.

He, Z., S. Yang, Y. Ju, and C. Sun, 2009, Microwave photocatalytic degradation of Rhodamine B using TiO2 supported on activated carbon: Mechanism implication: Journal of Environmental Sciences-China, v. 21, p. 268-272.

Hou, M., L. Liao, W. Zhang, X. Tang, H. Wan, and G. Yin, 2011, Degradation of rhodamine B by Fe(0)-based Fenton process with H2O2: Chemosphere, v. 83, p. 1279-1283.

Martinez-Huitle, C., E. dos Santos, D. de Araujo, and M. Panizza, 2012, Applicability of diamond electrode/anode to the electrochemical treatment of a real textile effluent: Journal of Electroanalytical Chemistry, v. 674, p. 103-107.

Merouani, S., O. Hamdaoui, F. Saoudi, and M. Chiha, 2010, Sonochemical degradation of Rhodamine B in aqueous phase: Effects of additives: Chemical Engineering Journal, v. 158, p. 550-557.

Miller, C., H. Yu, and T. Waite, 2013, Degradation of rhodamine B during visible light photocatalysis employing Ag@AgCl embedded on reduced graphene oxide: Colloids and Surfaces a-Physicochemical and Engineering Aspects, v. 435, p. 147-153.

Muthukumar, M., D. Sargunamani, and N. Selvakumar, 2005, Statistical analysis of the effect of aromatic, azo and sulphonic acid groups on decolouration of acid dye effluents using advanced oxidation processes: Dyes and Pigments, v. 65, p. 151-158.

Pandey, A., P. Singh, and L. Iyengar, 2007, Bacterial decolorization and degradation of azo dyes: International Biodeterioration & Biodegradation, v. 59, p. 73-84.

Panizza, M., and G. Cerisola, 2009a, Direct And Mediated Anodic Oxidation of Organic Pollutants: Chemical Reviews, v. 109, p. 6541-6569.

Panizza, M., and G. Cerisola, 2009b, Electro-Fenton degradation of synthetic dyes: Water Research, v. 43, p. 339-344.

Ramirez, C., A. Saldana, B. Hernandez, R. Acero, R. Guerra, S. Garcia-Segura, E. Brillas, and J. Peralta-Hernandez, 2013, Electrochemical oxidation of methyl orange azo dye at pilot flow plant using BDD technology: Journal of Industrial and Engineering Chemistry, v. 19, p. 571-579.

Rocha, J., A. Solano, N. Fernandes, D. da Silva, J. Peralta-Hernandez, and C. Martinez-Huitle, 2012, Electrochemical Degradation of Remazol Red BR and Novacron Blue C-D Dyes Using Diamond Electrode: Electrocatalysis, v. 3, p. 1-12.

Rodrigo, M. A., P. Cañizares, A. Sánchez-Carretero, and C. Sáez, 2010, Use of conductive-diamond electrochemical oxidation for wastewater treatment: Catalysis Today, v. 151, p. 173-177.

Saez, C., M. Panizza, M. A. Rodrigo, and G. Cerisola, 2007, Electrochemical incineration of dyes using a boron-doped diamond anode: Journal of Chemical Technology and Biotechnology, v. 82, p. 575-581.

Serrano, K., P. Michaud, C. Comninellis, and A. Savall, 2002, Electrochemical preparation of peroxodisulfuric acid using boron doped diamond thin film electrodes: Electrochimica Acta, v. 48, p. 431-436.

Sáez, C., M. A. Rodrigo, and P. Cañizares, 2008, Electrosynthesis of ferrates with diamond anodes: AIChE Journal, v. 54, p. 1600-1607.

Sánchez-Carretero, A., C. Sáez, P. Cañizares, and M. A. Rodrigo, 2011, Electrochemical production of perchlorates using conductive diamond electrolyses: Chemical Engineering Journal, v. 166, p. 710-714.

Tavares, M., L. da Silva, A. Solano, J. Tonholo, C. Martinez-Huitle, and C. Zanta, 2012, Electrochemical oxidation of Methyl Red using Ti/Ru0.3Ti0.7O2 and Ti/Pt anodes: Chemical Engineering Journal, v. 204, p. 141-150.

Vacca, A., M. Mascia, S. Palmas, and A. Da Pozzo, 2011, Electrochemical treatment of water containing chlorides under non-ideal flow conditions with BDD anodes: Journal of Applied Electrochemistry, v. 41, p. 1087-1097.

Figure Captions

Figure 1. Mineralization of Rhodamine B, as a function of Q, during electrolysis in different supporting electrolytes at two current densities (a) 60 mA cm^{-2} and (b) 120 mA cm^{-2}: ▲ Na_2SO_4; □ $HClO_4$; ■ H_3PO_4; △ NaCl.

Figure 2. Changes in the COD, as a function of Q, during electrolysis of Rhodamine solutions containing different supporting electrolytes at two current densities (a) 60 mA cm^{-2} and (b) 120 mA cm^{-2}: ▲ Na_2SO_4; □ $HClO_4$; ■ H_3PO_4; △ NaCl.

Figure 3. Influence of the current density on the first order kinetic constants for the CDEO of Rhodamine B: ▲ Na_2SO_4; □ $HClO_4$; ■ H_3PO_4; △ NaCl.

Figure 4. Instantanteous current efficiency constants for the electrolysis of Rhodamine B solutions in different supporting electrolyte media: ▲ Na_2SO_4; □ $HClO_4$; ■ H_3PO_4; △ NaCl.

Figure 5. Main intermediates detected, as a function of time, during the electrolysis of Rhodamine B solutions containing different supporting electrolytes ((a) $HClO_4$, (b) NaCl, (c) H_3PO_4 and (d) Na_2SO_4) at 60 mA cm^{-2}: phthalic acid (▲); 2,5-hydroxybenzoic acid (●); benzoic acid (■); 3-dinitrobenzoic acid (♦); α- hidroxyglutaric acid (△); intermediate 6 (○) and intermediate 7 (□)

Figure 6. Influence of the current density on the maximum concentration of intermediates detected during the electrolysis of Rhodamine B solutions containing different supporting electrolytes, (a) $HClO_4$, (b) NaCl, (c) H_3PO_4 and (d) Na_2SO_4:

438 phthalic acid (▲); 2,5-hydroxybenzoic acid (●); benzoic acid (■); 3-dinitrobenzoic acid

439 (♦); α- hidroxyglutaric acid (△); intermediate 6 (○) and intermediate 7 (□).

440

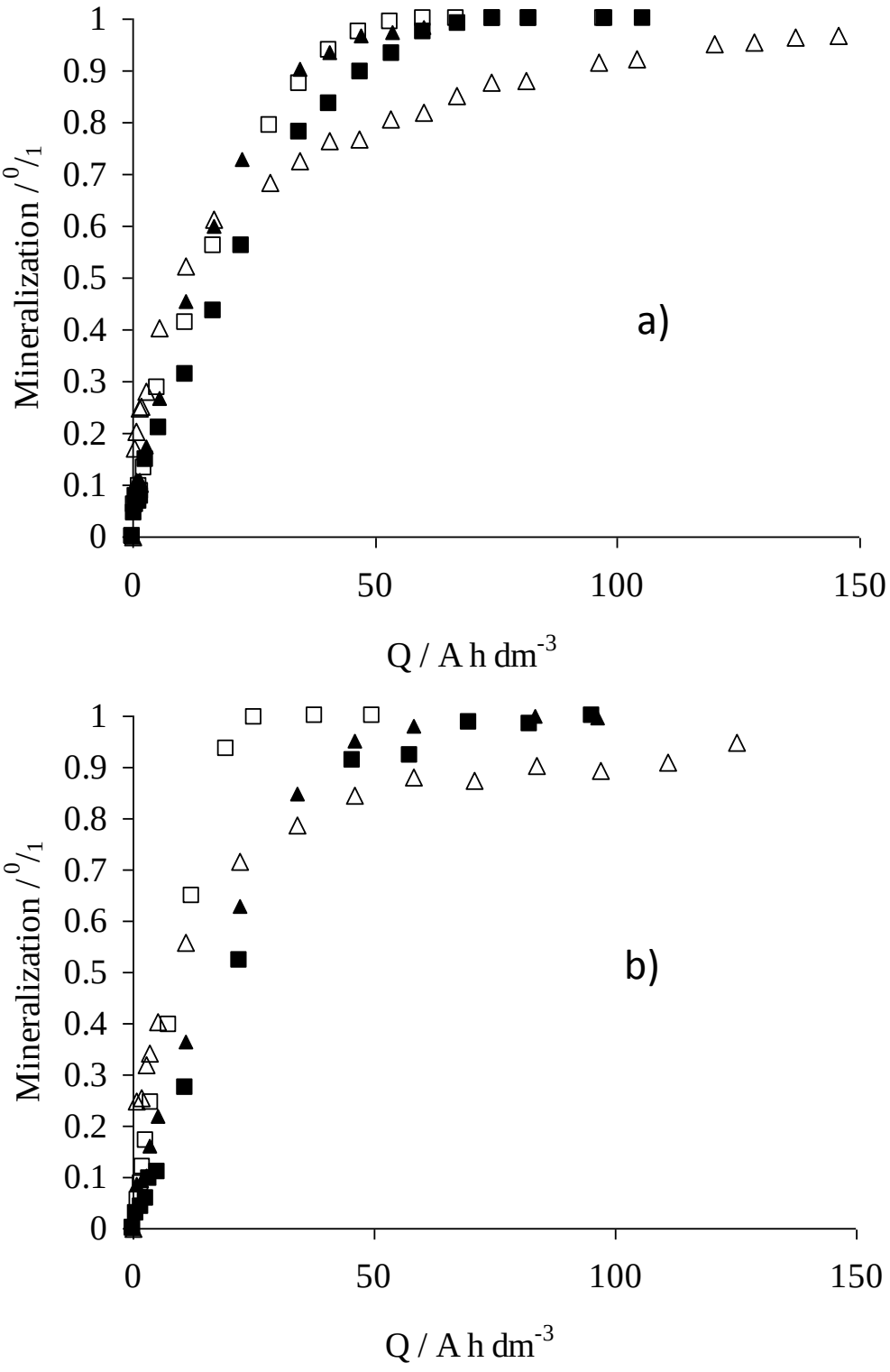
Mineralization / %
1
0.9
0.8
0.7
0.6
0.5
0.4
0.3
0.2
0.1
0
0
50
100
150
Q / A h dm-3
a)
Mineralization / %
1
0.9
0.8
0.7
0.6
0.5
0.4
0.3
0.2
0.1
0
0
50
100
150
Q / A h dm-3
b)

Figure 1

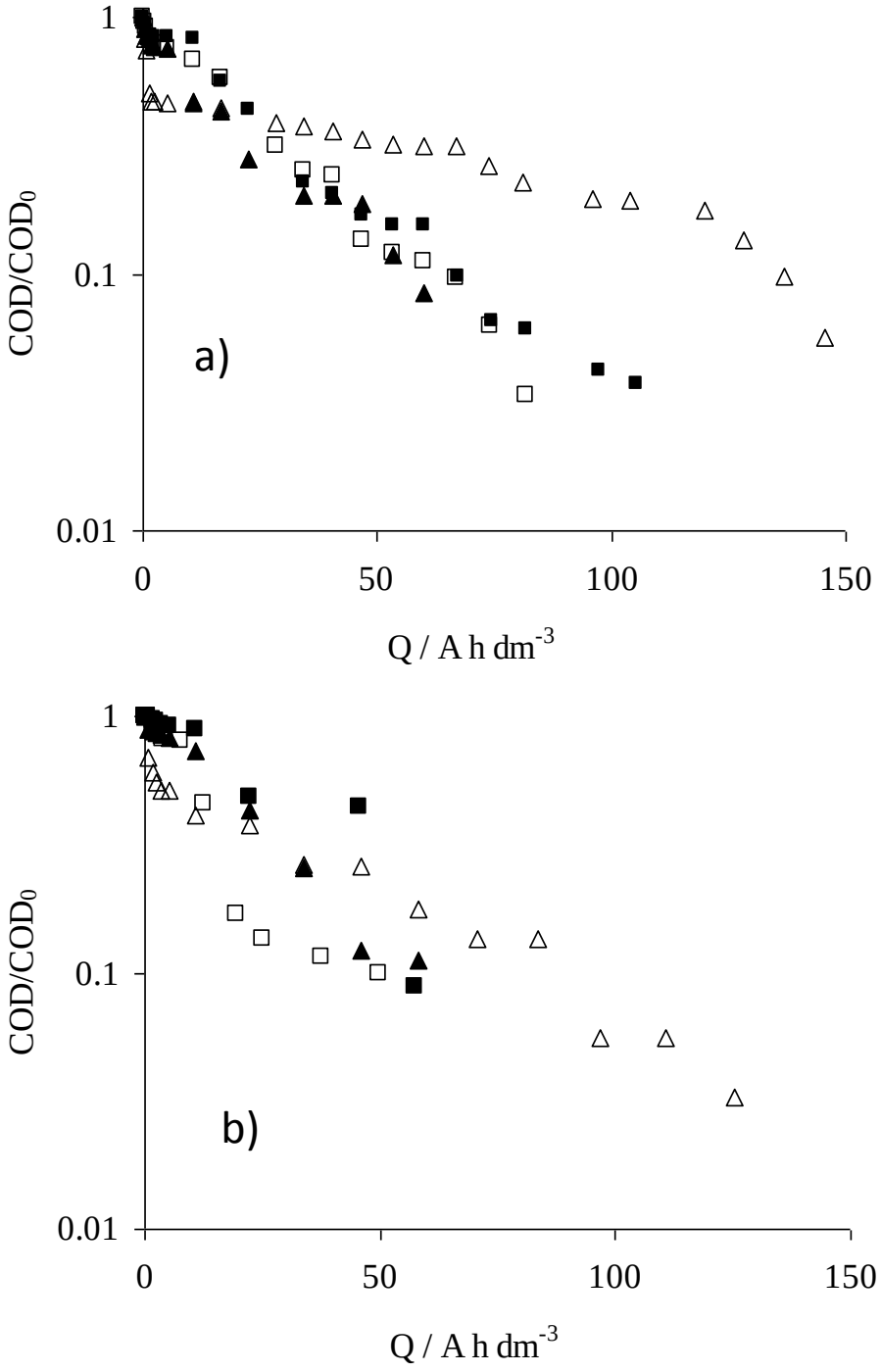
1
0.1
0.01
COD/COD0
a)
0
50
100
150
Q / A h dm-3
1
0.1
0.01
COD/COD0
b)
0
50
100
150
Q / A h dm-3

Figure 2

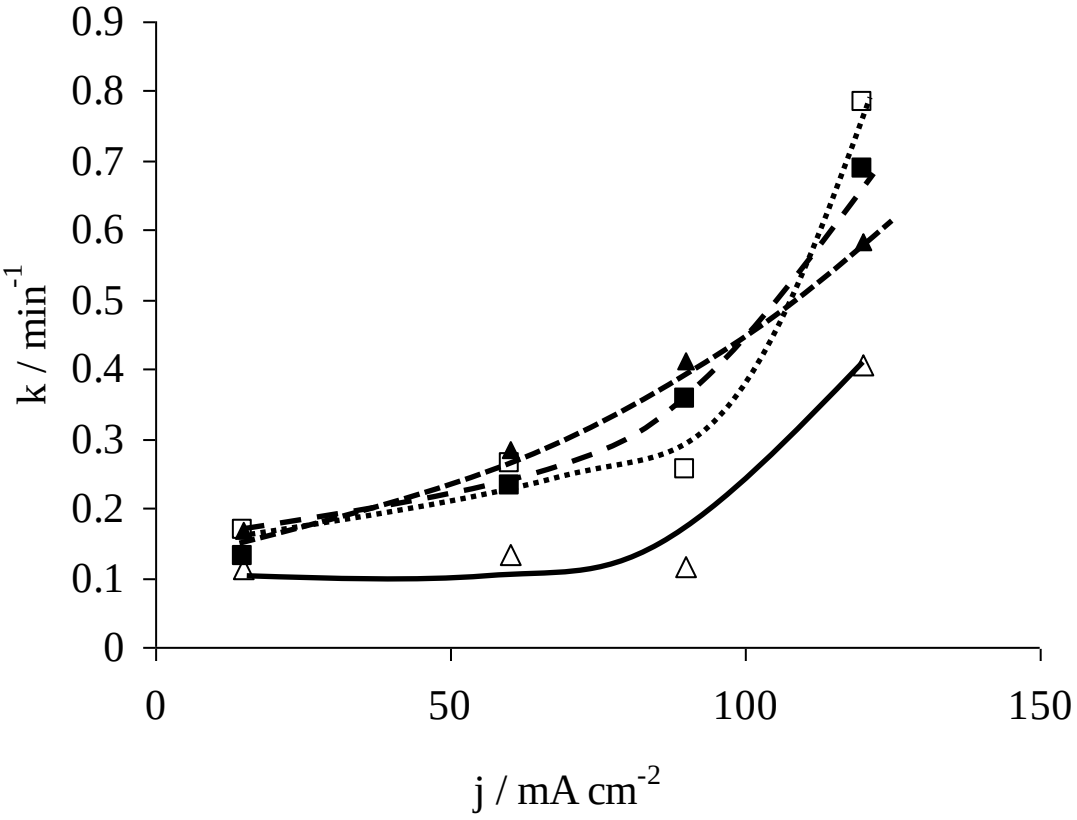

Figure 3

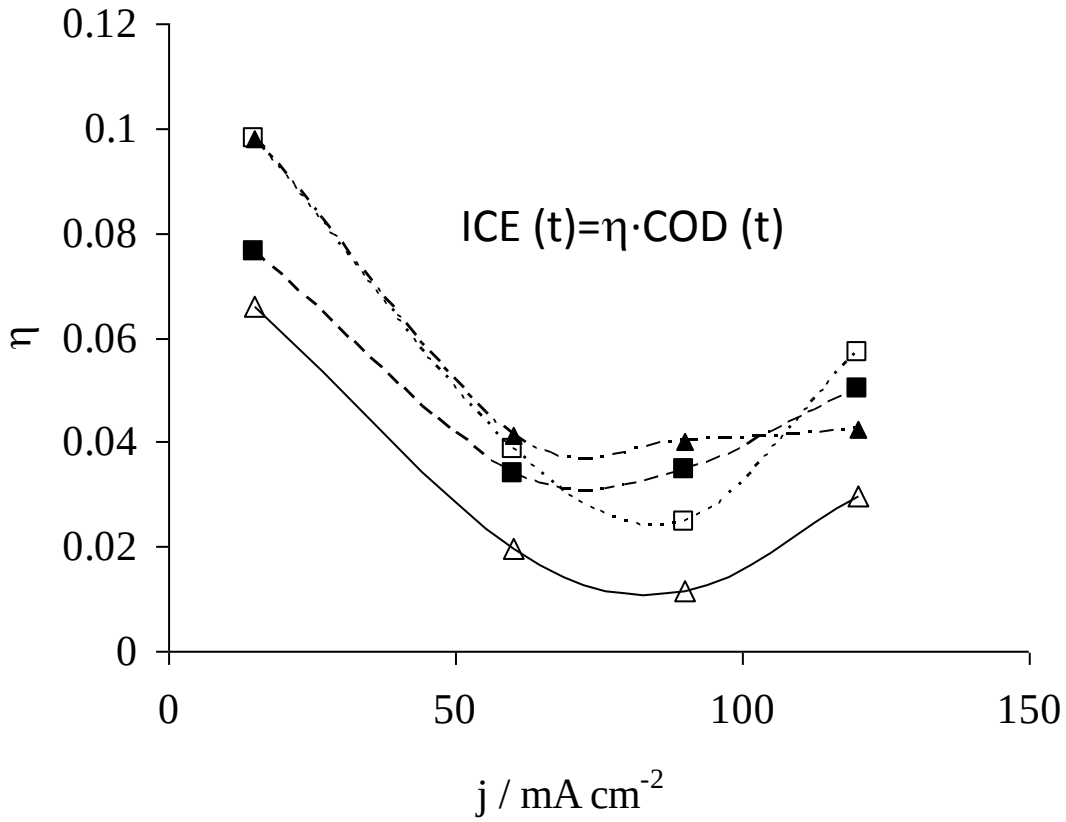

Figure 4

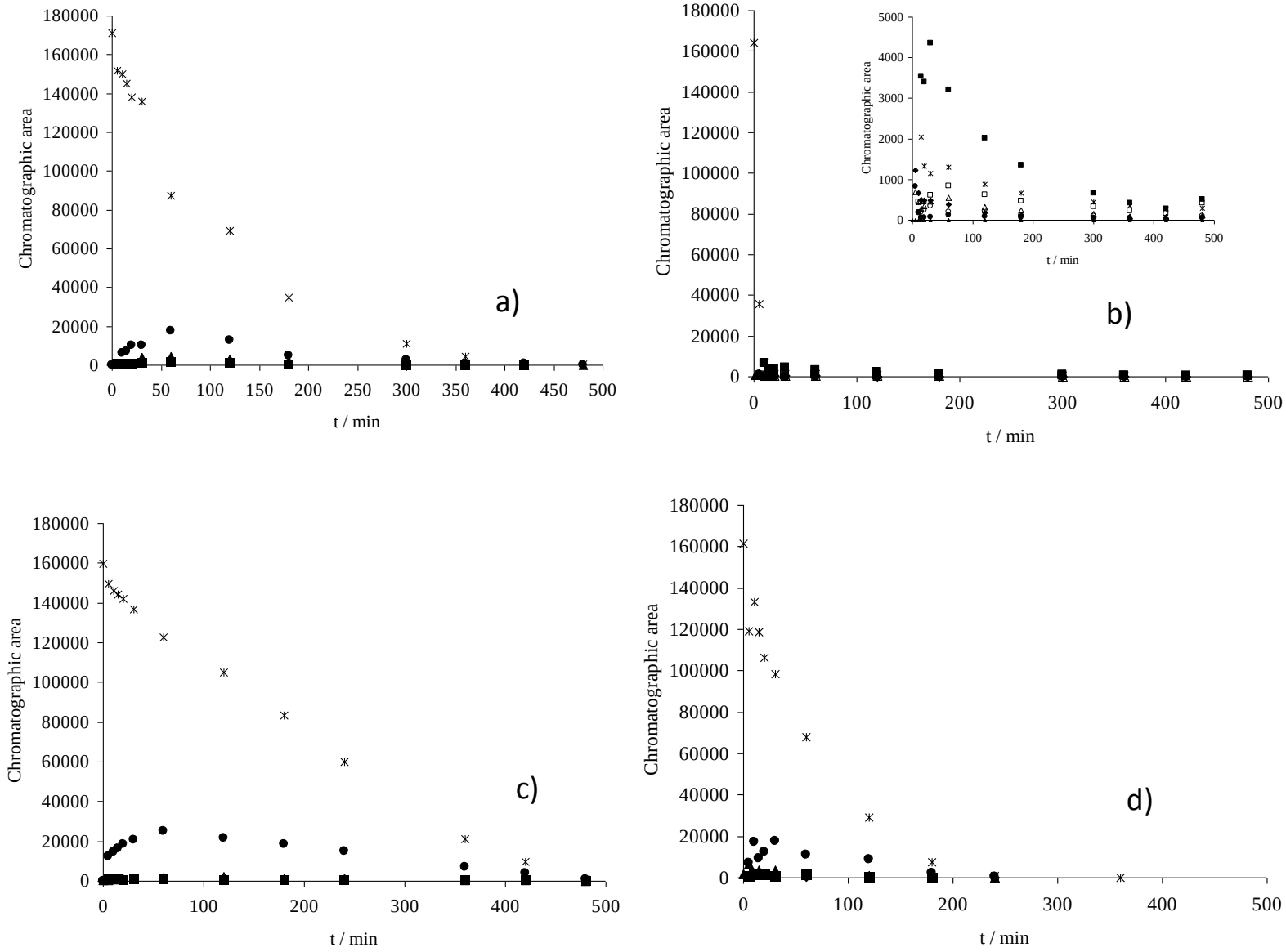

526

Figure 5

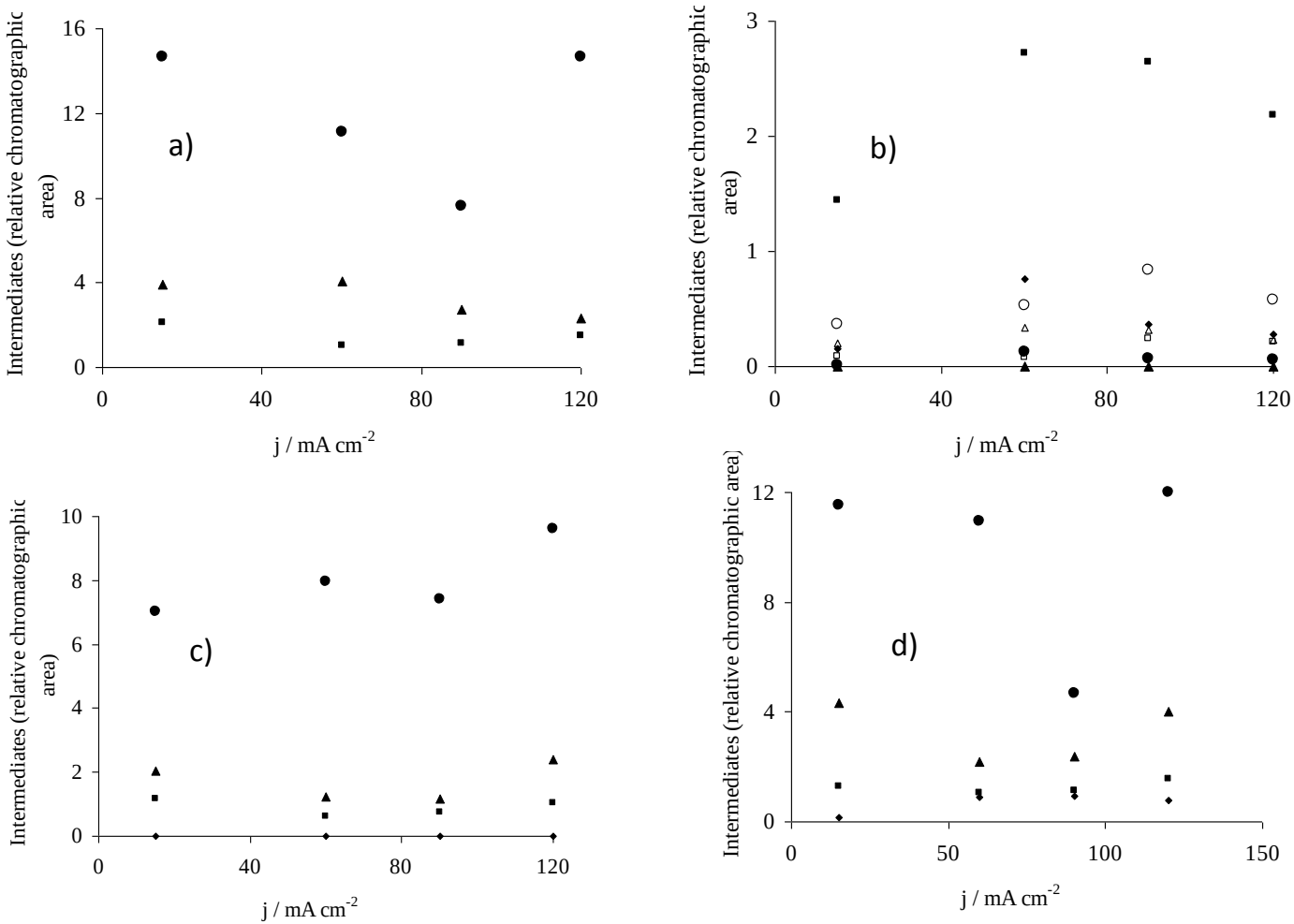

527

528

Figure 6

Figure 6